

Frustrated honeycomb-lattice bilayer quantum antiferromagnet in a magnetic field[☆]

Taras Krokhamlskii^{a,b}, Vasyl Baliha^{a,*}, Oleg Derzhko^{a,b,c}, Jörg Schulenburg^d, Johannes Richter^c

^a*Institute for Condensed Matter Physics, National Academy of Sciences of Ukraine, Svientsitskii Street 1, 79011 L'viv, Ukraine*

^b*Department for Theoretical Physics, Ivan Franko National University of L'viv, Drahomanov Street 12, 79005 L'viv, Ukraine*

^c*Institut für theoretische Physik, Otto-von-Guericke Universität Magdeburg, P.O. Box 4120, 39016 Magdeburg, Germany*

^d*Universitätsrechenzentrum, Otto-von-Guericke Universität Magdeburg, P.O. Box 4120, 39016 Magdeburg, Germany*

Abstract

Frustrated bilayer quantum magnets have attracted attention as flat-band spin systems with unconventional thermodynamic properties. We study the low-temperature properties of a frustrated honeycomb-lattice bilayer spin- $\frac{1}{2}$ isotropic (XXX) Heisenberg antiferromagnet in a magnetic field by means of an effective low-energy theory using exact diagonalizations and quantum Monte Carlo simulations. Our main focus is on the magnetization curve and the temperature dependence of the specific heat indicating a finite-temperature phase transition in high magnetic fields.

Keywords: quantum Heisenberg antiferromagnet, frustrated honeycomb-lattice bilayer, localized magnon, magnetothermodynamics

PACS: 75.10.-b, 75.10.Jm

1. Introduction

In the present paper, we consider a spin- $\frac{1}{2}$ antiferromagnetic Heisenberg model on a N -site two-dimensional lattice shown in Fig. 1. The Hamiltonian of the model reads

$$H = \sum_{\langle ij \rangle} J_{ij} \mathbf{s}_i \cdot \mathbf{s}_j - h S^z, \quad J_{ij} > 0, \quad S^z = \sum_i s_i^z. \quad (1)$$

The first sum in Eq. (1) runs over all bonds of the frustrated honeycomb-lattice bilayer, see Fig. 1, that is, J_{ij} acquires three values: J_2 (vertical red bonds), J_1 (nearest-neighbor intralayer black bonds), and J_X frustrating inter-

layer blue bonds). We are interested in the regime when J_2 is the strongest bond and a deviation of J_X from J_1 is small, or, more precisely, $J_2 > 3J$ with $J = (J_1 + J_X)/2$ and $|J_1 - J_X|/J_2 \ll 1$. If $J_1 = J_X$ one faces the so-called ideal frustration case characterized by a flat-one magnon band [1–3], otherwise the system is slightly away from the ideal frustration region in the parameter space.

The described model has attracted some interest recently from experimental and theoretical sides. On one hand, the interest in this model stems from experiments on $\text{Bi}_3\text{Mn}_4\text{O}_{12}(\text{NO}_3)$, in which the ions Mn^{4+} form a frustrated spin- $\frac{3}{2}$ bilayer honeycomb lattice [4–8]. On the other hand, there are a few theoretical papers considering the ground-state and low-temperature properties of a Heisenberg antiferromagnet on a frustrated bilayer honeycomb lattice [9–11], in which classical spin [9] or quantum spin- $\frac{1}{2}$ [10, 11] models in nonzero [9, 11] or zero [10] magnetic field were discussed using various complementary approaches. In particular, in our recent work [11] it has been shown that the localized-magnon picture [1–3],

[☆]O. D. and J. R. acknowledge the support by the Deutsche Forschungsgemeinschaft (project RI615/21-2). O. D. acknowledges the kind hospitality of the University of Magdeburg in April-May of 2017. T. K. and O. D. were partially supported by Project FF-30F (No. 0116U001539) from the Ministry of Education and Science of Ukraine.

*Corresponding author

Email address: baliha@icmp.lviv.ua (Vasyl Baliha)

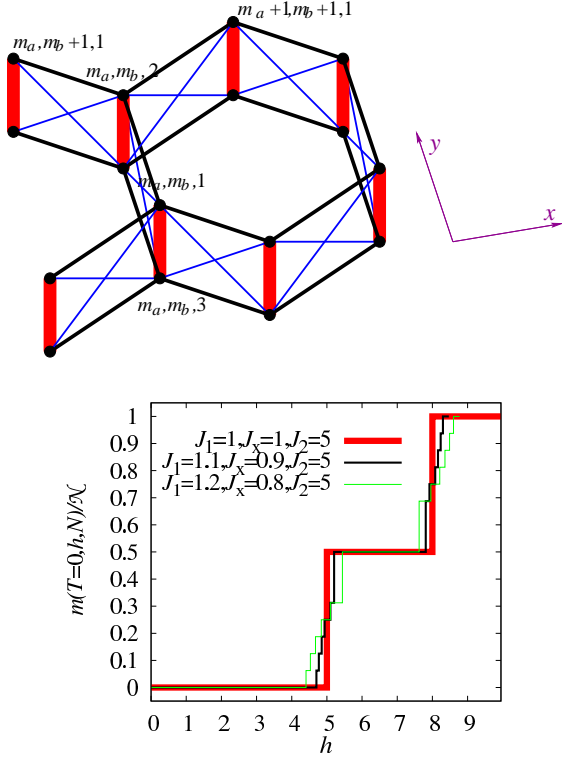


Figure 1: Top: the frustrated honeycomb-lattice bilayer studied in the present paper. The unit cell contains 4 sites and the corresponding Bravais lattice is the triangular lattice with basis vectors $\mathbf{a} = \sqrt{3}a_0\mathbf{i}$ and $\mathbf{b} = -\frac{\sqrt{3}}{2}a_0\mathbf{i} + \frac{3}{2}a_0\mathbf{j}$ (a_0 is the hexagon side length). The integer numbers m_a and m_b determine the position of the unit cell. The thick red vertical bonds represent the strongest interlayer coupling J_2 , the thin black bonds within each layer correspond to the nearest-neighbor intralayer coupling J_1 , and the thin blue bonds between the layers correspond to the frustrated interlayer coupling J_X . Bottom: exact-diagonalization data of the ground-state magnetization curve of a finite honeycomb-lattice bilayer of $N = 32$ sites for model (1) with $J_2 = 5$ and $J_1 = J_X = 1$ (thick red line), $J_1 = 1.1$, $J_X = 0.9$ (thin black line), $J_1 = 1.2$, $J_X = 0.8$ (very thin green line).

which emerges for the ideal frustration case, yields a simple effective description of the low-temperature thermodynamics in a moderate and strong magnetic field. Since in this regime only the two states on each vertical bond J_2 , $|u\rangle = |\uparrow\uparrow\rangle$ and $|d\rangle = \frac{1}{\sqrt{2}}(|\uparrow\downarrow\rangle - |\downarrow\uparrow\rangle)$ (localized magnon), dominate thermodynamic properties, it is not astonishing that the effective model is an antiferromagnetic honeycomb-lattice Ising model in a uniform magnetic field with the Hamiltonian $H_{\text{eff}} = C - h \sum_{m=1}^N T_m^z + \sum_{\langle mn \rangle} J^z T_m^z T_n^z$, where $\mathcal{N} = N/2$ and the (pseudo)spin- $\frac{1}{2}$ operators are defined as follows: $T^z = \frac{1}{2}(|u\rangle\langle u| - |d\rangle\langle d|)$, $T^+ = |u\rangle\langle d|$, and $T^- = |d\rangle\langle u|$. Moreover, slightly away from the ideal frustration case we arrive at an Ising-like XXZ Heisenberg antiferromagnet in an external field along the easy axis on the honeycomb lattice with the Hamiltonian

$$H_{\text{eff}} = C - h \sum_{m=1}^N T_m^z + \sum_{\langle mn \rangle} [J^z T_m^z T_n^z + J(T_m^x T_n^x + T_m^y T_n^y)],$$

$$C = \mathcal{N} \left(-\frac{h}{2} - \frac{J_2}{4} + \frac{3J}{8} \right), \quad J = \frac{J_1 + J_X}{2},$$

$$h = h - J_2 - \frac{3J}{2}, \quad J^z = J, \quad J = J_1 - J_X. \quad (2)$$

The effective model (2) was used in Ref. [11] to explain a peculiarity of the ground-state magnetization curve that is related to a spin-flop transition which is present in a two-dimensional Ising-like XXZ Heisenberg antiferromagnet in an external field along the easy axis. However, the magnetothermodynamics of the frustrated honeycomb-lattice bilayer quantum antiferromagnet (see Eq. (1) and Fig. 1), which can be examined on the basis of the effective model (2), was beyond the scope of that paper. Now we fill this gap and present results for some low-temperature thermodynamic quantities of the frustrated honeycomb-lattice bilayer quantum antiferromagnet in a magnetic field. It is important to note that, since the quantum spin model (1) is frustrated, a direct application of quantum Monte Carlo approach is impossible because of the infamous “sign problem”. However, this powerful method can be applied to the (unfrustrated) effective model (2) describing the low-energy degrees of freedom.

2. Magnetothermodynamics. Exact diagonalization and quantum Monte Carlo

We begin with testing the accuracy of the effective-model description (2). To this end, we consider the full initial model (1) on a finite bilayer lattice of $N = 24$ sites (see Fig. 3 in Ref. [11]) and perform exact-diagonalization calculations [12] to obtain thermodynamic quantities. Then we compare these findings with the results of the exact-diagonalization study of the corresponding effective model (2) of $N = 12$ sites. For concreteness, we fix the set of parameters as follows: $J_2 = 5$ and $J_1 = 1.1$, $J_X = 0.9$.

First we consider the magnetization curve $M(T, h)$ at zero temperature, see Fig. 1, bottom. In case of ideal frustration, i.e., $J_1 = J_X = 1$, the $M(h)/N$ curve is independent of the system size: M is zero until $h < h_2 = J_2 = 5$, it acquires one-half of the saturation value if $h_2 < h < h_{\text{sat}} = J_2 + 3J_1 = 8$, and achieves the saturation for $h > h_{\text{sat}}$ [11]. Deviations from the ideal frustration case lead to modifications around h_2 and h_{sat} , however, the wide plateaus are still present, see Fig. 1, bottom.

Next we report the temperature dependences of the magnetization and the specific heat for magnetic fields around the saturation field, see Fig. 2. It is in order to comment the applied exact-diagonalization approach. The total size of the Hamiltonian matrix for model (1) increases as S^z decreases and becomes beyond the present computational possibilities for $S^z < 5$ (even exploiting symmetries already for $S^z = 5$ we face a matrix of total size $57\,687 \times 57\,687$). Fortunately, for the system at hand near the saturation field, the subspaces with small S^z becomes relevant at high temperatures only. This is evident from the comparison of the results in Fig. 2 which account the subspaces with $S^z = 12, \dots, 5$ (solid lines) and the subspaces with $S^z = 12, \dots, 6$ (broken lines). Clearly, the exact-diagonalization data for the initial model (1) in Fig. 2 are reliable at least up to $T = 0.7$. Furthermore, effective-model predictions (symbols) reproduce perfectly all low-temperature features in Fig. 2 for temperatures until about $T = 0.5$. Clearly, the temperature region in which effective theory is accurate depends on the values of J_2 , J_1 , J_X , and h , however, the statement that the simpler (unfrustrated) effective model correctly describes low-energy degrees of freedom is not questioned. Concerning the temperature profiles of $M(T)$ and $C(T)$ shown in Fig. 2, a prominent feature is the in-

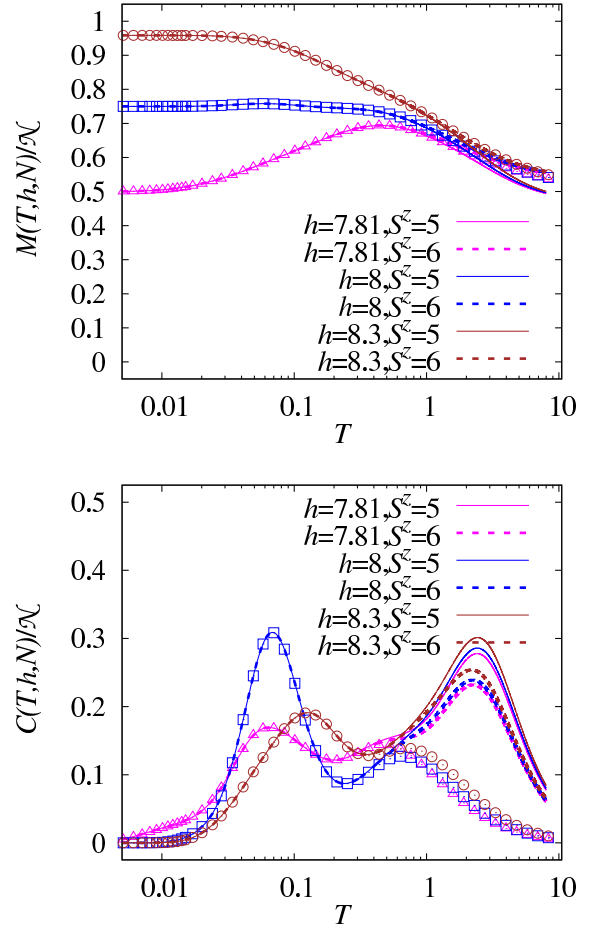


Figure 2: Magnetization (top) and specific heat (bottom) for the system at hand with $J_2 = 5$, $J_1 = 1.1$, and $J_X = 0.9$ at different fields $h = 7.81$ (magenta), $h = 8$ (blue), and $h = 8.3$ (brown). Exact-diagonalization results for initial model (1) of $N = 24$ sites (lines) are compared to exact-diagonalization results for effective model (2) of $N = 12$ sites (symbols).

crease of the magnetization as the temperature is growing as it is found for magnetic fields slightly below h_{sat} . That is related to a large manifold of low-lying states having larger values of total S^z than the ground state, and, these states become accessible as T increases. Another unconventional feature is the double-peak structure of the specific heat. Again, a large manifold of low-lying states is responsible, however, the value of the total S^z of these states is irrelevant for $C(T)$.

Having shown that the effective model works well at least up to $T = 0.5$, we perform quantum Monte Carlo calculations [13] and exact diagonalizations [12] for the (unfrustrated) effective model (2) considering much larger systems, see Fig. 3. The main peculiarity of the magnetization curve shown in Fig. 3 is related to a spin-flopping process present in model (2): antiferromagnetically interacting (pseudo)spins abruptly change their direction from parallel to perpendicular orientation with the respect to the easy axis of the anisotropic XXZ model (2) at some critical magnetic field h_c , where h_c is slightly above 7.8 for the considered set of parameters. In particular for quantum spins, this process discussed for the first time by Louis Néel in 1936, is not trivial at all depending on the lattice, spin value, temperature fluctuations etc. We are not aware of studies of the spin-flop phenomenon in the quantum Ising-like XXZ Heisenberg model on a honeycomb lattice (see, however, some related studies in Ref. [14–17]) and such a study goes beyond the scope of this short article. However, a number of features are obvious from the results reported in Fig. 3. Thus, at sufficiently low temperatures (say, below $T = 0.02$) the magnetization around h_c is hardly modified. But as temperature increases further, the value at which magnetization starts to grow rapidly becomes smaller and the slope of magnetization curve becomes smaller too. Finally, the magnetization becomes moderately rounded and at sufficiently high temperature (say, above $T = 0.1$) no traces of the spin-flop transition are visible. The temperature dependence of the specific heat exhibits a low-temperature maximum, see Figs. 2 and 3. Within the spin-flop phase, i.e., between h_c and h_{sat} , excitations are gapless, but they are gapped outside this field region. As a result, the curves $C(T, h, N)$ against T exhibit similar low-temperature behavior for h between h_c and h_{sat} and differ from such curves for h outside this field region, see the low-temperature region above $T = 0.02$. Furthermore, it

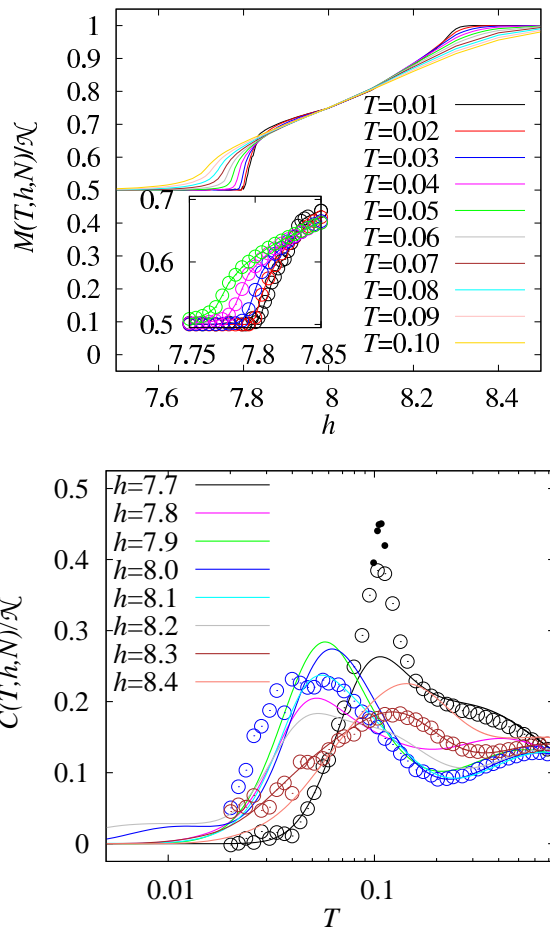


Figure 3: Magnetization curves at different temperatures (top) and temperature dependences of the specific heat at different fields (bottom) for $J_2 = 5$, $J_1 = 1.1$, and $J_X = 0.9$ as they follow from quantum Monte Carlo simulations (N up to 2304, top panel and N up to 1024, circles in the bottom panel) and exact diagonalizations ($N = 18$, solid lines in the bottom panel) for effective model (2). All curves $C(T, h, N)/N \rightarrow 0$ with $T \rightarrow 0$ as it should be.

is interesting to compare $C(T)$ profiles for $h = 7.7$ and $h = 8.0$ in Fig. 3. While the former one reflects a transition from the antiferromagnetic to paramagnetic phase, the latter one reflects a transition from the spin-flop to paramagnetic phase [16]. Noticeable finite-size effects for $h = 7.7$ (large empty circles correspond to $N = 256$ whereas small filled circles correspond to $N = 1024$) indicate a singularity which emerges in the thermodynamic limit [11]. In contrast, the temperature-driven transition between the spin-flop and paramagnetic phase is not accompanied by a specific-heat singularity. These traces of the spin-flop phase are expected to be seen for the initial model in the considered parameter region.

3. Conclusions

In this paper, we have demonstrated that the effective model (2) can be used to describe the low-temperature thermodynamics of the frustrated honeycomb-lattice bilayer quantum antiferromagnet (1) around the ideal frustration regime when $J_2 > 3(J_1 + J_X)/2$ and $|J_1 - J_X|/J_2 \ll 1$. If deviations from the ideal frustration regime are present (i.e., for $J_1 \neq J_X$), the magnetization jump transforms into a spin-flop transition and the model exhibits interesting low-temperature properties related to the arisen spin-flop phase. Remarkably, the spin-flop physics emerges in the $spin-\frac{1}{2}$ isotropic (i.e., XXX) Heisenberg antiferromagnet (1), without any explicit anisotropy, only due to the lattice geometry and the specific values of exchange couplings J_{ij} .

Concerning experimental realizations of the frustrated honeycomb-lattice bilayer spin system, the magnetic compound $\text{Bi}_3\text{Mn}_4\text{O}_{12}(\text{NO}_3)$ is a candidate, although, the exchange parameters of the spin Hamiltonian for $\text{Bi}_3\text{Mn}_4\text{O}_{12}(\text{NO}_3)$ are still under debate [7, 8], and it might happen the J_2 does not have sufficient strength. The search for other honeycomb materials, where our findings would be observable, is desirable and is encouraged.

References

References

[1] J. Schulenburg, A. Honecker, J. Schnack, J. Richter, H.-J. Schmidt, Phys. Rev. Lett. 88 (2002) 167207.

[2] M. E. Zhitomirsky, H. Tsunetsugu, Phys. Rev. B 70 (2004) 100403; O. Derzhko, J. Richter, Phys. Rev. B 70 (2004) 104415.

[3] O. Derzhko, J. Richter, M. Maksymenko, Int. J. Mod. Phys. B 29 (2015) 1530007.

[4] O. Smirnova, M. Azuma, N. Kumada, Y. Kusano, M. Matsuda, Y. Shimakawa, T. Takei, Y. Yonesaki, N. Kinomura, J. Am. Chem. Soc. 131 (2009) 8313.

[5] S. Okubo, F. Elmasry, W. Zhang, M. Fujisawa, T. Sakurai, H. Ohta, M. Azuma, O. A. Sumirnova, N. Kumada, J. Phys.: Conf. Ser. 200 (2010) 022042.

[6] M. Matsuda, M. Azuma, M. Tokunaga, Y. Shimakawa, N. Kumada, Phys. Rev. Lett. 105 (2010) 187201.

[7] H. C. Kandpal, J. van den Brink, Phys. Rev. B 83 (2011) 140412(R).

[8] M. Alaei, H. Mosadeq, I. A. Sarsari, F. Shahbazi, arXiv:1702.05255.

[9] F. A. Gómez Albarracín, H. D. Rosales, Phys. Rev. B 93 (2016) 144413.

[10] H. Zhang, C. A. Lamas, M. Arlego, W. Brenig, Phys. Rev. B 93 (2016) 235150.

[11] T. Krokhumalskii, V. Baliha, O. Derzhko, J. Schulenburg, J. Richter, Phys. Rev. B 95 (2017) 094419.

[12] J. Richter, J. Schulenburg, Eur. Phys. J. B 73 (2010) 117; <https://www-e.uni-magdeburg.de/jschulen/spin/>

[13] A. F. Albuquerque *et al.* (ALPS collaboration), J. Magn. Magn. Mater. 310 (2007) 1187; B. Bauer *et al.* (ALPS collaboration), J. Stat. Mech. (2011) P05001.

[14] M. Kohno, M. Takahashi, Phys. Rev. B 56 (1997) 3212.

[15] S. Yunoki, Phys. Rev. B 65 (2002) 092402.

[16] M. Holschneider, S. Wessel, W. Selke, Phys. Rev. B 75 (2007) 224417; W. Selke, M. Holschneider, R. Leidl, S. Wessel, G. Bannasch, D. Peters, Physics Procedia 6 (2010) 84.

- [17] K. Balamurugan, S.-H. Lee, J.-S. Kim, J.-M. Ok, Y.-J. Jo, Y.-M. Song, S.-A. Kim, E. S. Choi, M. D. Le, J.-G. Park, Phys. Rev. B 90 (2014) 104412.